High-Pressure Molecular Phases of Solid Carbon Dioxide

S. A. Bonev, F. Gygi, T. Ogitsu, and G. Galli

Lawrence Livermore National Laboratory, University of California, Livermore, California 94550, USA

(Received 21 December 2002; published 7 August 2003)

We present a theoretical study of solid CO_2 up to 50 GPa and 1500 K using first-principles calculations. In this pressure-temperature range, interpretations of recent experiments have suggested the existence of CO_2 phases which are intermediate between molecular and covalent-bonded solids. We reexamine the concept of intermediate phases in the CO_2 phase diagram and propose instead molecular structures, which provide an excellent agreement with measurements.

DOI: 10.1103/PhysRevLett.91.065501 PACS numbers: 62.50.+p, 61.50.Ah, 64.70.Kb, 78.30.–j

Understanding the evolution of the bonding properties of molecular crystals as a function of pressure is a fundamental question in condensed matter physics. Recently, this question has received widespread attention due to key progress in experimental techniques and hence, the availability of new data for a number of molecular solids [1]. In the case of CO_2, the interest has been further intensified due to its importance for planetary science and technical applications. However, despite several experimental investigations of the CO_2 high-pressure phases, the changes of intra- and intermolecular bonds, as well as of electronic and vibrational properties, as a function of pressure are not yet well understood. In addition, large portions of the CO_2 phase diagram are unexplored from a theoretical standpoint.

At low-pressure P and temperature T, CO_2 condenses as a molecular solid in the cubic $Pa3$ structure (known as dry ice, phase I), which is characterized by strong double bonds (C═O distance of 1.16 Å) and rather weak intermolecular interactions [2]. Recently, a high-P and high-T phase of CO_2 (phase V) has been discovered [3–7], which is completely different from the molecular solid. It has a polymeric quartzlike structure, and a very low compressibility (the experimentally derived bulk modulus B_0 is 365 GPa). Following this exciting discovery, two additional new phases have been reported [8–10] experimentally (II and IV in Fig. 1), both of which were credited with unusual properties; their structures were described as intermediate between that of molecular and covalently bonded crystals.

In this Letter, we present a study of the CO_2 phase diagram based on first-principles density functional theory (DFT) calculations. Our results challenge the interpretation of CO_2-II, III, and IV as exhibiting dramatic differences in the nature of the molecular bonding with respect to the low-pressure molecular crystal. In place of the previously proposed structures for CO_2-II and IV, we suggest new, molecular ones. We demonstrate that in addition to being stable, our newly proposed structures give results in excellent agreement with measurements and provide a consistent explanation of experimental observations.

At ambient T, CO_2-I undergoes a pressure-induced transformation to the orthorhombic $Cmca$ symmetry (phase III) between 12 and 22 GPa [3,11–17]. The exact nature of this transition and the structure of phase III are still unsettled; experimental studies have suggested a region of coexistence between CO_2-I and III [15], and also an intermediate distorted low-T phase [17]. Furthermore, it was reported [9] that the I to III transition is strongly temperature dependent, becoming abrupt above 400 K, and that CO_2-III may actually be metastable. The two newly discovered phases II and IV are believed to be thermodynamically stable and quenchable. It was proposed that CO_2-II has the $P4_2/mnm$ symmetry with elongated C═O bonds, 1.33 Å, reduced intermolecular distances below 2.38 Å (hence named associated or dimeric phase), and $B_0 = 131$ GPa [9,10]. CO_2-IV was described as $Pbcn$, with C═O bonds as long as 1.53 Å, and bent (O═C═O angle of 160°) and strongly (dipole) interacting molecules [8]. Such remarkable properties would imply that CO_2 is losing its molecular character in a "gradual" way, a concept promoted as a key for understanding its phase diagram in analogy with solids such as N_2O and SiO_2. In addition, CO_2-III, despite having a stable C═O bond, was also assigned a B_0 as high as 87 GPa [9]. The stability of the proposed bent and associated phases, and the unusual bulk properties of CO_2-II, III, and IV have not been investigated theoretically to date.

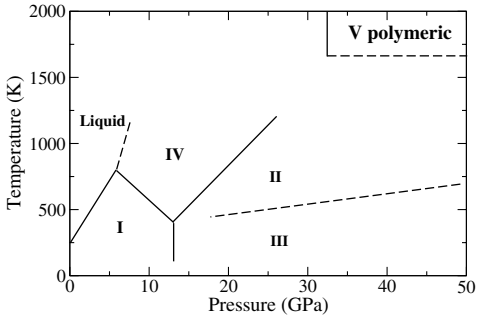

FIG. 1. Phase diagram of CO_2 according to Ref. [9], where CO_2-III ($Cmca$) is reported to be metastable.

 0031-9007/03/91(6)/065501(4)$20.00

We performed a series of first-principles calculations, including full structural optimizations, phonon spectra, and free energies, in order to study the stability and properties of the phases proposed experimentally up to 50 GPa and 1500 K. The DFT calculations were carried out within the Perdew-Burke-Ernzerhof [18] generalized gradient approximation (GGA) using the ABINIT code [19], which implements plane-wave basis sets [20].

First, we have examined the stability of the dimeric and bent structures for phases II and IV. Starting from the previously proposed $P4_2/mnm$ and $Pbcn$ with elongated molecular bonds, we carried *full* structural optimizations at various pressures up to 50 GPa. In all cases, upon relaxing the atomic coordinates the C═O bond lengths decreased by about 15% and 30% for $P4_2/mnm$ and $Pbcn$, respectively, to become comparable to the free CO_2 molecule [21]. In the case of $Pbcn$, the O═C═O angle also straightened to 180°. The energy differences between the theoretically stable molecular structures and the associated and bent phases are, respectively, more than 3 and 6 eV per molecule. These are energy scales corresponding to the breaking of a covalent bond. They are beyond the errors of the GGA and present strong evidence that the previously proposed bent and dimeric structures are not stable. In order to further investigate this issue, we examine below published experimental data for CO_2-II, III, and IV, and demonstrate that they can be explained in terms of two *stable* structures, $Cmca$ and $P4_2/mnm$, which are *strictly molecular*.

Computed equation of state (EOS) at $T = 0$ for the three molecular structures $Pa3$, $Cmca$, and $P4_2/mnm$ is reported in Fig. 2, along with the available experimental data. In all three cases, the calculated EOS agrees very well with the measured one; the computed PV curves fall within the experimental uncertainties. We find about 2% relative volume reduction from $Pa3$ to $Cmca$ [22] above 30 GPa and another 0.5% from $Cmca$ to $P4_2/mnm$ (see the inset in Fig. 2). Yoo *et al.* reported a ~5%–7% volume decrease associated with the III to II transition; however, they also observed lattice strain in their phase III samples [9], which may explain the difference between their results and ours. Furthermore, the PV curve of $Cmca$ comes close to and eventually merges with that of $Pa3$ below 20 GPa in agreement with Aoki *et al.* [15]. Thus, the measured EOS data are reproduced well despite the lack of molecular association in our optimized $P4_2/mnm$. The computed EOS parameters are summarized in Table I together with values derived from experiment [23]. The agreement is good for $Pa3$, but there is an order of magnitude difference for the values of B_0 of $Cmca$ and $P4_2/mnm$. Since we are using the same EOS fit as Ref. [10], and we in fact agree very well with the *direct* PV measurements, the large difference likely comes from extrapolating the experimental data, spread above 20 GPa, down to ambient pressure.

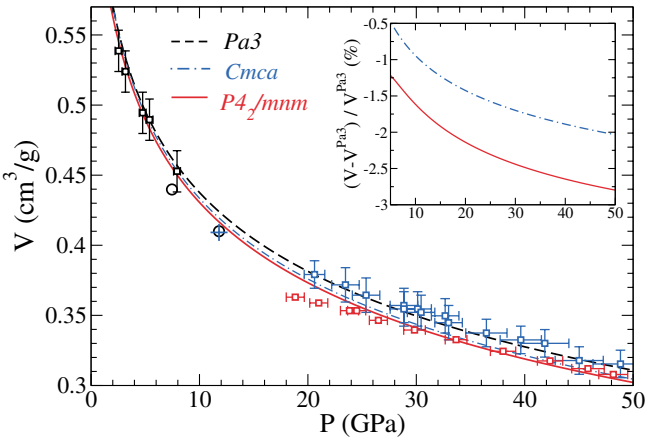

FIG. 2 (color). Pressure-volume dependence of selected CO_2 structures: $Pa3$ (black), $Cmca$ (blue), and $P4_2/mnm$ (red). The lines are *ab initio* calculations; the points indicate experimental data from Refs. [3,10] (squares), and Ref. [15] (circles and a plus). The inset shows calculated reduction in volume of $P4_2/mnm$ and $Cmca$ relative to $Pa3$.

The published experimental evidence invoked to propose that CO_2-II exhibits the properties of a dimeric polymorph consists of: (i) a large splitting of the internal symmetric stretching mode, ν_1 [9], (ii) a broad librational mode identified as B_{1g} [9,10], and (iii) powder x-ray diffraction measurements [10]. We carried out calculations of the vibron spectrum [24] of *molecular* $P4_2/mnm$ and $Cmca$ as a function of P. A plot of ν_1 in Fig. 3(a) shows that the measured splitting, as well as the relative values for $P4_2/mnm$ and $Cmca$, are reproduced remarkably well by the theoretical structures. Yoo *et al.* assumed that the large vibron splitting observed in CO_2-II is evidence for decreased intermolecular distances; our results indicate that the crystal field in the molecular $P4_2/mnm$ is sufficient to explain the splitting. One should note that phonons are calculated as a second derivative of the energy; therefore the agreement with experimental frequencies within meV, as found here, is a strong indication that computed total energies and forces are extremely accurate.

The computed pressure dependence of the Raman-active external modes of the three theoretical structures is shown in Fig. 3(b). The agreement with experiment [17] is again good, though our values are consistently slightly

TABLE I. Equation of state parameters for selected CO_2 phases. The theoretical data are well fitted to a third-order Birch-Murnaghan equation of state.

Structure	V_0 (cm^3/g)	B_0 (GPa)	B_0'	Ref.
$Pa3$	0.714	2.93	7.8	[11]
$Pa3$	0.726	3.21	8.10	This study
$Cmca$	0.450	87	3.3	[10]
$Cmca$	0.725	3.53	7.12	This study
$P4_2/mnm$	0.408	131	2.1	[10]
$P4_2/mnm$	0.701	4.37	6.66	This study

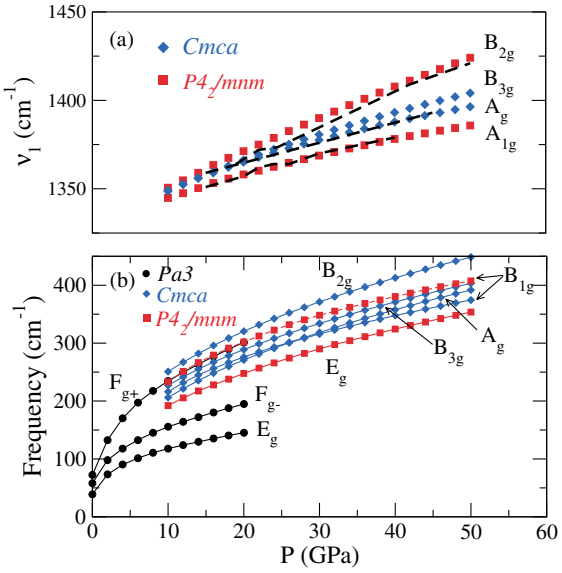

FIG. 3 (color). Computed Raman-active modes (solid symbols) of the theoretically stable structures. (a) Symmetric stretching vibron. Dashed lines indicate experimental data from [9]; they are from a Fermi resonance band, and have been shifted by 52 cm^{-1} for comparison. (b) External modes.

lower than the measured ones. The experimental frequencies of the two Raman-active modes of CO_2-II at 19 GPa are about 260 and 320 cm^{-1}—the former being a broad peak—and were classified as B_{1g} and E_g, respectively [9,10]. The broad mode was previously associated with dynamical disorder in the lattice. The molecular $P4_2/mnm$ has modes with frequencies 245 and 300 cm^{-1} at this P; however, it is the degenerate E_g which has the lower frequency, and therefore corresponds to the experimentally observed broad peak. Its broadening can be explained by invoking a lifting of the E_g degeneracy when the tetragonal cell is deformed into an orthorhombic one (resulting in the *Pnnm* symmetry). Such a distortion is consistent with the x-ray data reported in Ref. [10] and we estimate that between 20 and 30 GPa there is 10 cm^{-1} splitting for every 1% modifiaction of a and b.

We now turn our attention to the x-ray analysis. In $P4_2/mnm$, the atomic positions are C(2a) at [0, 0, 0], and O(4f) at [x, x, 0]. The dimeric phase, according to Ref. [10], corresponds to $x = 0.2732$, while our stable structure corresponds to $x = 0.23075$, i.e., $x \approx 0.25 \pm \delta$ for the two structures, where $\delta = 0.02$. Among the observed diffraction peaks, only the (101) and (211) reflections depend on the sign of δ. Their measured intensities relative to the calculated intensities of the same reflections are in ratios of 2.3 and 0.3 for the dimeric, and 0.4 and 1.8 for the molecular structures, respectively. We therefore conclude that at present the diffraction measurements are insufficient to distinguish between the dimeric and the molecular $P4_2/mnm$ structures.

Finally, we examine the relative stability of all considered crystal structures as a function of both P and T. A plot of enthalpies showing that *Cmca* is never thermodynamically stable at low T is reported in Fig. 4(a). This finding confirms a previous observation [4] that the orthorhombic symmetry obtained during ambient T compression of CO_2-I is metastable; the reason why the system reverts to it is the low kinetic barrier associated with the rotation of the molecules from their alignment in *Pa*3 to that in *Cmca*. In additional support of this conclusion, we have performed structural optimizations starting from the *Pbca* structure, and relaxing the atomic coordinates. The *Pbca* lattice is obtained from *Pa*3 by deforming the cubic cell; further rotations of the molecules in the y-z plane then lead to *Cmca*. In all such calculations above 15 GPa, the CO_2 molecules quickly align in the y-z plane, thus ending up in the *Cmca*, rather than in the energetically favorable $P4_2/mnm$ phase. This happens regardless of whether the unit cell is tetragonal or orthorhombic; the deformation of $P4_2/mnm$ to the orthorhombic *Pnnm* costs only about 1 meV per molecule for 1% distortion of a and b.

The kinetic barrier between *Cmca* and $P4_2/mnm$ can be overcome by heating the system above ambient T. Interestingly, we find that upon further heating at constant P there is a *thermodynamic* phase boundary above which the orthorhombic phase is now *stable*. The phonon free energies, computed as described in Ref. [24], are

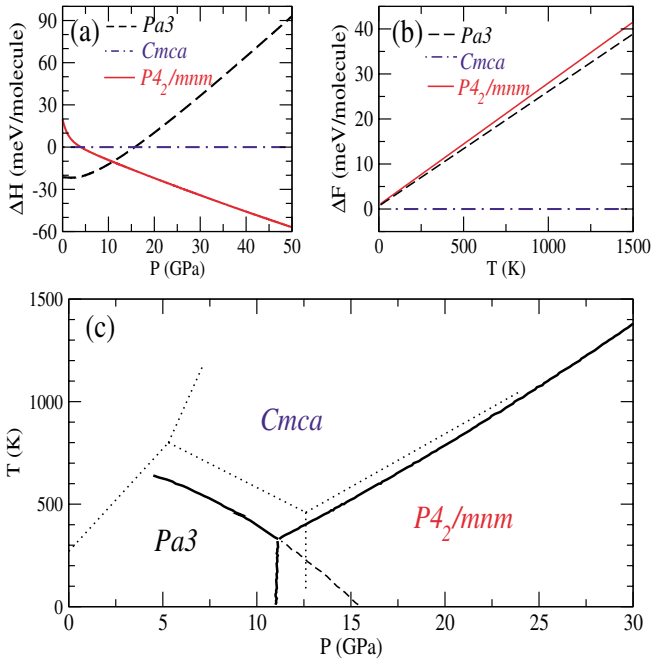

FIG. 4 (color). (a) Enthalpy versus P relative to the *Cmca* phase at $T = 0$. (b) Phonon free energy versus T relative to the *Cmca* structure at 16 GPa; the reported differences do not vary strongly with P. (c) Relative stability of selected CO_2 structures from Gibbs free energy comparison (solid lines); here P includes phonon contributions. Dotted lines are the experimental phase constraints from Ref. [9] (see Fig. 1), and the dashed line is an extension of the *Pa*3-*Cmca* phase boundary.

plotted in Fig. 4(b). The transition to *Cmca* is entropy driven and is mainly due to a soft acoustic phonon mode. Its physical origin is in the specific geometry of *Cmca*, allowing for a relatively unobstructed shearlike motion parallel to the *y* axis; we have confirmed this by sampling the potential surface with frozen-phonon calculations.

The computed stability regions for $Pa3$, $P4_2/mnm$, and *Cmca* are shown in Fig. 4(c). Since we are comparing the relative stability of a *limited* number of structures, we cannot firmly conclude that Fig. 4(c) represents the actual phase diagram of CO_2. However, the almost perfect matching of the stability region of *Cmca* with that of CO_2-IV makes the identification between the two phases rather compelling. We note that a phase IV of CO_2 was first suggested by Olijnyk and Jephcoat [17] based on the observed multiplicity of external Raman-active modes between 10 and 20 GPa, at ambient T. Their data are consistent with the Raman spectrum of $Pa3$, *Cmca*, and *Pbca*. As we discussed above, *Pbca* is intermediate between $Pa3$ and *Cmca*, and may be present close to the boundary of stability between these two phases, which extends from 5 to 16 GPa in our calculations. In addition, *Cmca* has a soft (below 100 cm^{-1} at ~20 GPa) zone-boundary libron, B_{1g}, tilting the molecules away from the *y*-*z* plane, which crosses two of the acoustic modes. Thus, when excited at high T, *Cmca* could actually turn into a peculiar distorted phase. Reference [17] observed a similar distorted phase with a weak (otherwise forbidden) Raman activity of the bending internal mode, which they related to the presence of pressure inhomogeneities in the sample. We find such an explanation of the Raman activity observed by Yoo *et al.* [8] around 650 cm^{-1} more plausible than the existence of bent molecules.

In conclusion, we have presented a new interpretation of experimental data recently obtained for CO_2-II, III, and IV. Our *ab inito* calculations identify CO_2-II as a *molecular* structure with the $P4_2/mnm$ symmetry. We have also elucidated the high-T behavior of molecular CO_2, and have found the *Cmca* symmetry to be preferable due to its relatively large entropy. Based on our findings, we propose that measurements of the high-T phase IV be interpreted along the lines of an orthorhombic, and possibly distorted, molecular phase. Finally, we note that the external Raman modes of several CO_2 structures are very close in frequency (see Fig. 3), and therefore may not be sufficient to discriminate between different phases.

We thank C. S. Yoo, J. Park, and V. Iota for useful discussions. This work was performed under the auspices of the U.S. Department of Energy at the University of California/LLNL under Contract No. W-7405-Eng-48.

[1] See, for example, R. J. Hemley, Annu. Rev. Phys. Chem. **51**, 763 (2000), and references therein.
[2] W. H. Keesom and J. W. L. Kohler, Physica (Amsterdam) **1**, 655 (1934); P. W. Bridgeman, Proc. Am. Acad. Arts Sci. **72**, 207 (1938); R. C. Hanson and L. H. Jones, J. Chem. Phys. **75**, 1102 (1981); B. Olinger, J. Chem. Phys. **77**, 6255 (1982).
[3] C. S. Yoo *et al.*, Phys. Rev. Lett. **83**, 5527 (1999).
[4] V. Iota, C. S. Yoo, and H. Cynn, Science **283**, 1510 (1999).
[5] S. Serra *et al.*, Science **284**, 788 (1999).
[6] J. Dong *et al.*, Phys. Rev. B **61**, 5967 (2000); **61**, 5967 (2000); Science **287**, 11a (2000).
[7] B. Holm *et al.*, Phys. Rev. Lett. **85**, 1258 (2000).
[8] C. S. Yoo, V. Iota, and H. Cynn, Phys. Rev. Lett. **86**, 444 (2001); Bull. Am. Phys. Soc. **48**, 914 (2003).
[9] V. Iota and C. S. Yoo, Phys. Rev. Lett. **86**, 5922 (2001).
[10] C. S. Yoo *et al.*, Phys. Rev. B **65**, 104103 (2002).
[11] L. Liu, Earth Planet Sci. Lett. **71**, 104 (1984).
[12] R. C. Hanson, J. Phys. Chem. **89**, 4499 (1985).
[13] B. Kuchta and R. D. Etters, Phys. Rev. B **38**, 6265 (1988); **47**, 14 691 (1993).
[14] K. Aoki, H. Yamawaki, and M. Sakashita, Phys. Rev. B **48**, 9231 (1993).
[15] K. Aoki *et al.*, Science **263**, 356 (1994).
[16] R. Lu and A. M. Hofmeister, Phys. Rev. B **52**, 3985 (1995).
[17] H. Olijnyk and A. P. Jephcoat, Phys. Rev. B **57**, 879 (1998).
[18] J. P. Perdew, K. Burke, and M. Ernzerhof, Phys. Rev. Lett. **77**, 3865 (1996).
[19] The ABINIT code is a common project of the Université Catholique de Louvain, Corning Incorporated, and other contributors (http://www.abinit.org).
[20] We used nonlocal pseudopotentials (s, p, and d angular momentum projections) of the Troullier-Martins type [N. Troullier and J. L. Martins, Phys. Rev. B **43**, 1993 (1991)]. A 45 Ha plane-wave cutoff and $4 \times 4 \times 4$ Monkhorst-Pack (MP) grids were found sufficient for energy, pressure, and bond length converged better than 1 meV/molecule, 5×10^{-3} GPa, and 10^{-3} Å, respectively. We obtained a very accurate description of the free molecule (bond length and harmonic vibrational frequency within 0.5% and 1.5% of the experimental values, respectively) and of the $Pa3$ crystal structure.
[21] In the case of $P4_2/mnm$, the bond length is 1.154 Å at 28 GPa, and eventually reduces to 1.148 Å at 50 GPa.
[22] Our optimized *Cmca* structure differs slightly from the one reported experimentally [15] and agrees with previous theoretical works [F. Gygi, Comput. Mater. Sci. **10**, 63 (1998); see also Ref. [5]].
[23] The values of these parameters are sensitive to the choice of the functional form used to fit the energy as a function of volume, as observed for other solids. A single set of PV data can be well fit with different combinations of B_0 and B_0'; see, for example, N. R. Keskar *et al.*, Phys. Rev. B **44**, 4081 (1991). Nevertheless, their relative values are qualitatively the same irrespective of the fit.
[24] Phonon computations were carried out in the harmonic approximation using the linear response method: S. Baroni, P. Giannozzi, and A. Testa, Phys. Rev. Lett. **58**, 1861 (1987); X. Gonze, Phys. Rev. B **55**, 10 337 (1997); **55**, 10 355 (1997); **56**, 7321 (1997); **51**, 8610 (1995). For phonon free energies, dynamical matrices were computed on a 64 point MP grid, corresponding to a real space cell containing 384 atoms (768 for $Pa3$).